Association of Petroleum Geologists. India
Registered under Societies Registration Act,No. 21 of 1860

GEO India 2022

Characterization of pore pressure and fracture gradient in the ultradeep water Cauvery Basin, India

Devendra Pote[1], P.R.Mishra, Sampad Mohanta, Souvik Sen
[1]Email: pote_devendra@ongc.co.in, Oil and Natural Gas Corporation Limited

Abstract

Understanding of subsurface pore pressure and fracture gradients is critical to design and execute drilling with optimum mud and casing policies. In this study we analyzed two exploratory wells drilled in the ultradeep water Cauvery Basin. The overburden gradient varies between 17.19 - 18.76 MPa/km. The Tertiary interval is observed to be hydrostatically pressured while the post-rift Upper Cretaceous shales are mildly overpressured with maximum pore pressure reaching up to 9.6 ppg before regressing to a lower level within the underlying late syn-rift sediments. Compaction disequilibrium is interpreted as the dominant overpressure generating mechanism in the study area. Fracture gradient is inferred from the available leak-off tests which exhibited an effective stress ratio of 0.53-0.59. The results of this study will be valuable for planning and execution of the future wells in the deep and ultradeep water Cauvery Basin.

Introduction

Pore pressure and fracture gradients are important input parameters for well planning as these serves as the minimum and maximum allowable downhole mud weight limit to avoid kick and loss scenarios. Assessment of these two are more critical in deep water and ultradeep water environments, which may consist of very narrow mud windows. This study is focused on the offshore Cauvery Basin, situated along the passive eastern margin of India. It extends from north of Pondicherry in the north to the Cape Comorin of the south. The basin is characterized by several NE-SW trending horst and graben structures, formed during initial rifting phase in late Jurassic to early Cretaceous. Initially, the grabens were filled with fluvial sediments, after which marine deposition became predominant, especially during the post-rift stage (Saha et al., 2019). Hydrocarbon pools have been discovered in all the sub basins of Cauvery Basin with the reservoirs ranging in age from Precambrian (basement) to Oligocene. Drilling activity has largely been concentrated near the Basement highs and their flanks. Very few wells were drilled targeting deeper syn-rift sequences.

A few previous works focused on the pore pressure and geomechanical aspects of Cauvery Basin (Dasgupta et al., 2016; Singh et al., 2017; Saha et al., 2019). However most of those are from the onshore or shallow offshore areas, which sets the premise of this work. We studied two ultradeep water exploratory wells which targeted the late syn-rift to post-rift Cretaceous targets. Tentative locations of these wells are presented in Figure 1. Well-A was drilled in a water depth of 1743m and has a TD of 5736m (from MSL), while Well-B was drilled till 5800m in a water depth of 2392m. Wireline data consisting of gamma ray, resistivity, bulk-density and compressional sonic slowness logs were available from both wells along with various downhole measurements (LOT, MDT), drilling information (casing shoe depth, mud weight etc.) and mudlog (cutting description, gas chromatography etc.). All these dataset were integrated in this study. The primary objectives of this work were: i) to estimate overburden pressure gradient, ii) identify pore pressure distribution across the encountered stratigraphy, ii) understand the reason of overpressure, and iv) distribution of fracture pressure gradients.

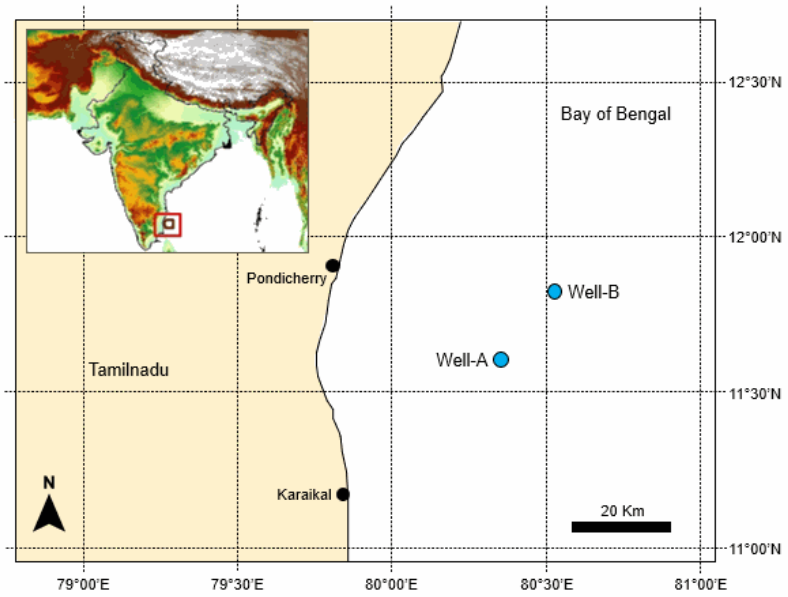

Figure 1: Location map of the two studied exploratory wells in the offshore Cauvery Basin.

Estimation of Overburden, pore pressure and fracture gradients

Here we briefly discuss the steps to estimate the three principal outputs of this work: vertical stress or overburden stress gradient (OBG), pore pressure (PP) and fracture gradient (FG). Estimation of OBG was straight forward, by using bulk-density log. Since the top section was not logged, we generated pseudo-density profile using Amoco relationship, which was then combined with the wireline log to generate a composite density profile before using it for OB calculation. Pore pressure (PP) against shales can be estimated by resistivity and compressional sonic slowness (DT). In this study, DT was used to infer PP by employing the Zhang (2011) model. The equation is as follows:

$$PP = OBG - (OBG-Phyd) * [\{\ln(DTml-DTm) - \ln(DT-DTm)\} / (c*Z)] \quad \ldots\ldots\ldots\ldots (1)$$

Where, Phyd is the hydrostatic pressure, DTml is the DT log value at mud line, DTm is the matrix slowness value, Z indicates depth. The parameter 'c' is the normal compaction parameter which is obtained from the following normal compaction trendline (NCT) of transit time (Zhang et al., 2020):

$$DTn = DTm + (DTml - DTm)\, e^{(-cZ)} \quad \ldots\ldots\ldots\ldots\ldots\ldots (2)$$

Where, DTn is the DT value along NCT. We have utilized downhole MDT measurements against the target reservoir intervals as well as drilling mud weight information (as proxy) to interpret the PP profiles in the studied wells. Fracture pressure gradient (FG) was determined using effective stress ratio (k)-based approach (Matthews and Kelly 1967). The equation is as follow:

$$FG = k\,(OBG - PP) + PP \quad \ldots\ldots\ldots\ldots\ldots (3)$$

Where, 'k' is inferred from Leak-off tests recorded at casing shoes.

Results and discussions

The Amoco pseudo-density profiles for both the wells were established considering a seabed sediment density of ~1.7 gm/cc and Amoco coefficient of 0.6. These set of parameters provided a satisfactory trend of the synthetic density when compared with the wireline bulk-density logs. At well TD of 5735m in the Well-A, the estimated OBG value is 16 ppg, while the Well-B has a 14.7 ppg overburden gradient at 5787m (TD~5800m). This translates to a 0.83 PSI/ft or 18.76 MPa/km vertical stress gradient in the Well-A, while Well-B displays a slightly lower OBG of 0.76 PSI/ft or 17.19 MPa/km contributed by higher water depth.

We generated a cross plot between sonic and density to understand the PP mechanism. Figure 2 indicated an overall linear relationship between these two which is indicative of either normal compaction or under-compaction, also known as compaction disequilibrium. With this understanding we confidently employed the trendline-based approach for the PP estimation. A depth vs. shale porosity cross plot for the two studied wells is presented in Figure 3. Here we have only plotted the shale porosities, while the shales were distinguished based on the gamma ray log primarily, supported by drill cutting information (available from mud logs).

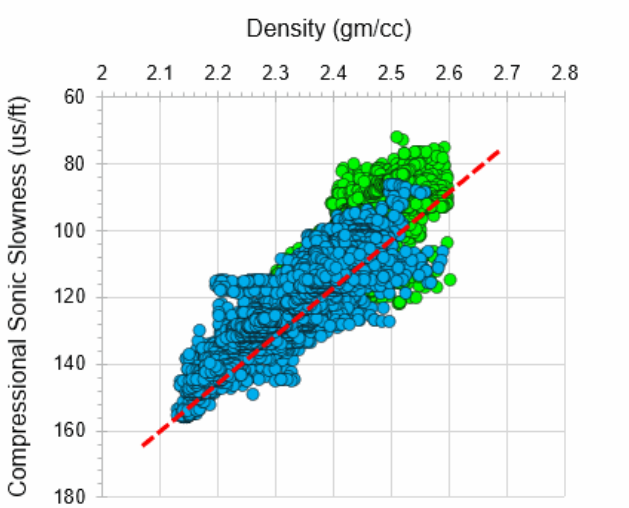

Figure 2: Cross plot between sonic compressional slowness and bulk-density for Well-A (blue circles) and Well-B (green circles).

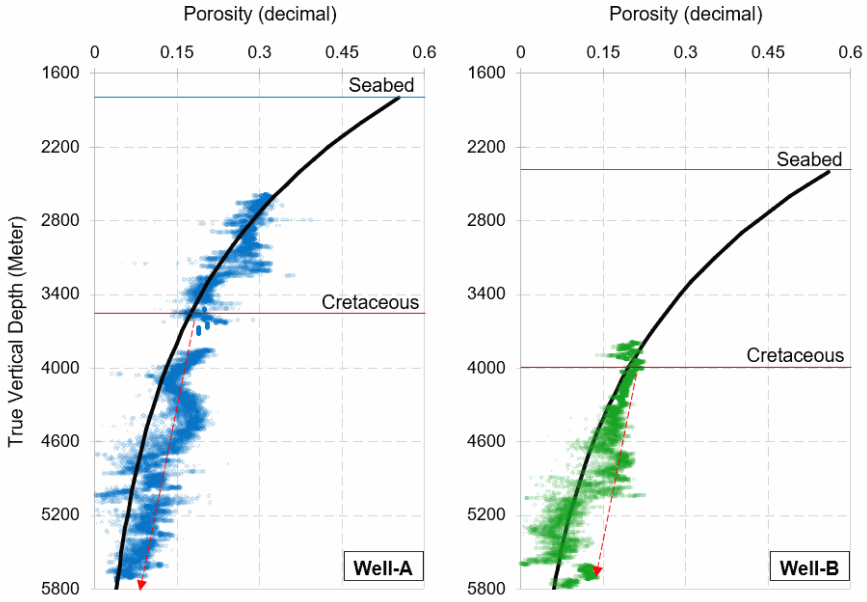

Figure 3: Depth vs porosity cross plot for the studied wells indicating porosities deviating from the trendlines tentatively from Cretaceous top.

Shale porosities of both the wells indicate a deviation from the porosity compaction trendline around at the top of Cretaceous and thereafter exhibit slightly higher values consistently. This behaviour is indicative of compaction disequilibrium mechanism. Due to higher sedimentation rate, the Cretaceous sediments possibly retained excess pore fluid generating overpressure. This porosity compaction trend was translated to a sonic NCT using Equation (2) where we considered a mudline slowness of ~200 µs/ft and a matrix slowness value of 53 µs/ft. With these values, a compaction parameter 'c' value of 0.0005 was observed to be best fitting, which was used for both the wells to estimate PP using Equation (1).

The calculated PP for both the wells are presented in Figure 4. Since deep resistivity data was unavailable for the entire well, this work utilized DT-based PP model. The final PP profile was interpreted by combining MDT measurements with the DT-based model outputs, which indicates a hydrostatic pore pressure of ~8.5 ppg in the entire Tertiary sequence in both the wells. The clay-dominated top 1200m of the post-rift Cretaceous interval (3600-4800m) in the Well-A indicates the shale pore pressure increasing from 8.5 ppg to a maximum value of 9.6 ppg. The lower part of the Cretaceous in Well-A consists of late syn-rift sandstone dominated sequence. Based on the MDT measurements, PP in this lower interval is interpreted as ~9.2 ppg.

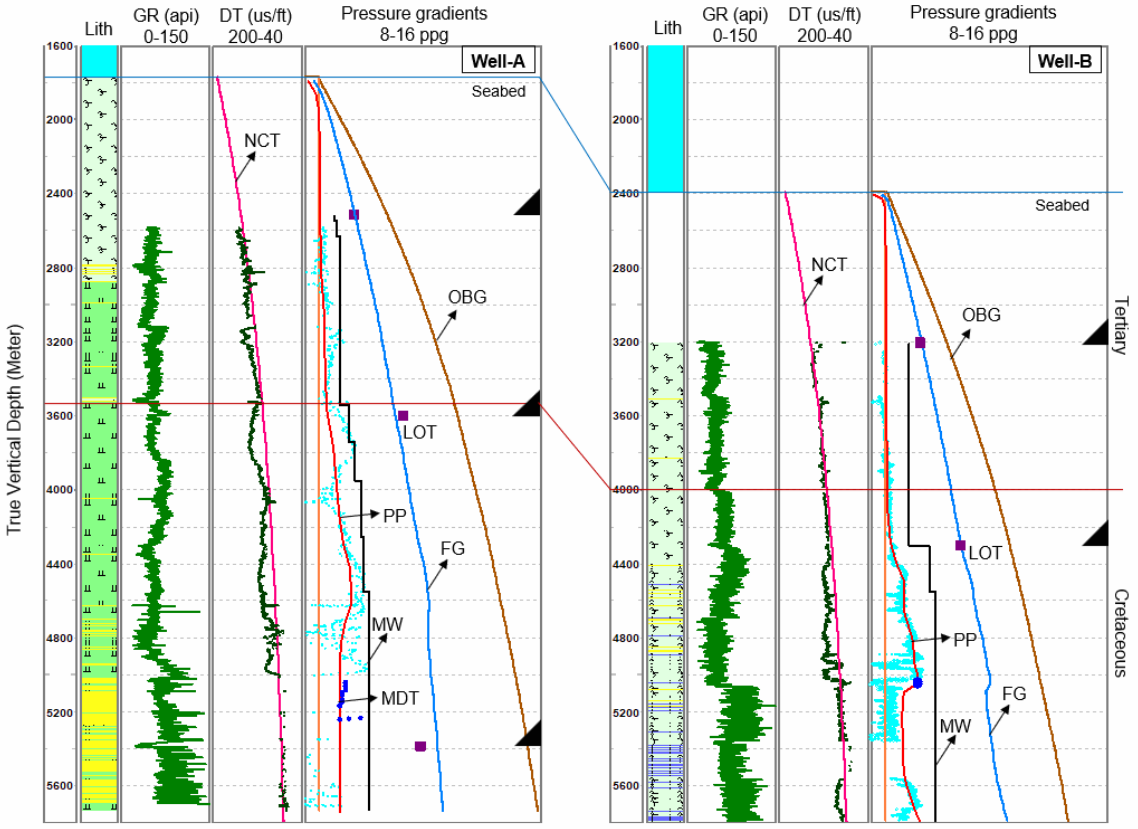

Figure 4: Interpreted sonic compaction trendline and estimated pressure gradients in the studied offshore wells

Similar pore pressure behaviour was also exhibited by the Cretaceous interval of Well-B, where the upper Cretaceous post-rift shales attain a maximum PP of 9.6 ppg and then regress to a lower value (9.2-9.4 ppg) in the late syn-rift interval lying in the bottom, which is unlike of Well-A, a more of limestone dominated in Well-B (Figure 4). These slightly overpressured Cretaceous intervals of both the studied wells were successfully drilled with a maximum mud weight of 10.2 ppg and the drilling reports did not mention any occurrence of formation fluid influx or connection gases indicating that the drilling mud weight was sufficiently overbalanced with respect to the formation pore pressure. For the estimation of FG we interpreted effective stress ratio (k) from the LOT data. Well-A had three LOT measurements which exhibited an average k value of 0.53. The two LOT measurements in the Well-B provided a slightly higher 'k' of ~0.59. Accordingly the fracture pressure gradients are generated (Figure 4).

Conclusions

Overburden pressure, pore pressure and fracture pressure gradients have been estimated from the two exploratory wells in Cauvery Basin. The mild over pressure zones are encountered in the upper Cretaceous post-rift intervals which possibly experienced a faster sedimentation rate. This is the first ever reporting pore pressure and fracture gradient distribution from the ultradeep water Cauvery Basin. The interpreted pressure gradients provide critical understanding of the available downhole drilling mud window. The results of this work will be beneficial to prepare the predrill pore pressure models and design casing as well as mud properties in the upcoming wells in the block.

Acknowledgement

Authors express their sincere gratitude to ONGC for providing the data and permission to present the work. Authors acknowledge the *Pore pressure module* of GEO Suite of software by Geologix Limited which was utilized for the analysis presented in this work.

References

Dasgupta, S., Chatterjee, R. and Mohanty, S.P., 2016, Predicton of pore pressure and fracture pressure in Cauvery and Krishna-Godavari basins, India, Marine and Petroleum Geology, vol.78, pp.493-506.

Matthews, W.R. and Kelly, J.,1967, How to predict formation pressure and fracture gradient, Oil Gas Journal, vol.65, pp.92-106.

Saha, S., Gariya, B.C., Panda, D., Perumulla, S., Podder, T., Thanvi, S. and Deshpande, C., 2019, Integration of 1D geomechanics modeling and high performance water-based mud HPWBM system design, improving cost-effective drilling of high-angle wells through Cauvery Shale sequence: A case study from Cauvery Basin, offshore India, SPE Oil and Gas India Conference and Exhibition, Mumbai, April 9-11, SPE-194626.

Singh, S., Palathoti, D., Chattopadhyay, T., Avadhani, V.L.N. and Deo, P.P., 2017, Deciphering present day stress through new generation image logs in Cauvery Basin, 4th SPWLA0India Symposium and Exhibition, February 11-12.

Zhang, J., Zheng, H., Wang, G., Liu, Z., Qi, Y., Huang, Z. and Fan, X., 2020, In-situ stresses, abnormal pore pressures and their impacts on the Triassic Xujiahe reservoirs in tectonically active western Sichuan basin, Marine and Petroleum Geology, vol. 122, 104708.

Zhang, J., 2011, Pore pressure prediction from well logs: methods, modifications, and new approaches, Earth Science Reviews, vol.108, pp.50–63.